Chapter 19
The Role of Nuclear Medicine in the Diagnosis of Amyloidosis

Claudio Tinoco Mesquita, Simone Cristina Soares Brandão, and Adriana Pereira Glavam

19.1 Introduction

Amyloidosis is a systemic infiltrative disease and when cardiac involvement is present, the prognosis is always poorer. Cardiac Amyloidosis (CA) is characterized by the extracellular deposition of misfolded proteins which aggregate as amyloid fibrils. The most predominant types of CA are amyloid immunoglobulin light chain (AL) and amyloid transthyretin (ATTR). The latter is further subtyped into hereditary (ATTRv), which results from protein mutations, and wild type, in the past known as senile type (ATTRw) [1].

The diagnosis of CA remains challenging. Endomyocardial biopsy is still considered the gold standard for diagnosing CA. Nevertheless, significant improvements in noninvasive imaging methods have led to fewer cases where biopsies are required [2–6]. In this scenario, nuclear medicine has achieved a central role. Currently, myocardial scintigraphy with bone-seeking tracers is the only noninvasive method

C. T. Mesquita
Nuclear Medicine and Molecular Imaging Department, Pró-Cardíaco Hospital, Rio de Janeiro, RJ, Brazil

Radiology Department, Federal Fluminense University, Rio de Janeiro, Brazil
e-mail: claudiotinocomesquita@id.uff.br

S. C. S. Brandão (✉)
Department of Medicine, Hospital das Clínicas, Universidade Federal de Pernambuco, Recife, Pernambuco, Brazil
e-mail: simone.brandao@ufpe.br

A. P. Glavam
Instituto Nacional de Cardiologia, Rio de Janeiro, RJ, Brazil

Hospital Copa Star, Rio de Janeiro, RJ, Brazil

Clínica de Diagnóstico por Imagem CDPI/DASA, Rio de Janeiro, RJ, Brazil

D. Xavier de Ávila, H. Villacorta Junior (eds.), *Amyloidosis and Fabry Disease*,
https://doi.org/10.1007/978-3-031-17759-0_19

capable of differentiating ATTR CA from AL CA which represents a paradigm shift in diagnosis. It is important to highlight that although scintigraphy has become a cornerstone of ATTR CA diagnosis, it must be evaluated in concomitance to monoclonal gammopathies test results [7]. Positron emission tomography associated with computed tomography (PET/CT) has also emerged as a potential noninvasive method to assess amyloid burden and response to treatment [8].

In this chapter, the authors propose a review of the current role of nuclear medicine in the diagnosis and prognosis of ATTR CA alongside a discussion about future directions in this promising field.

19.2 Imaging Targets in Cardiac Amyloidosis

Amyloid deposits in the myocardium interstice are the imaging direct targets to diagnose, prognose, and type CA. It consists of insoluble b-pleated sheets of fibrils formed from misfolded precursor proteins, as well as non-fibrillar components of serum amyloid P (SAP), glycosaminoglycans, and calcium [4–9].

Nuclear medicine methods act on a molecular level and can directly (PET/CT) or indirectly (scintigraphy and PET/CT) identify amyloid deposits, even before structural and functional changes can be observed on echocardiography or Cardiac Magnetic Resonance (CMR). Early diagnosis impacts prognosis and nuclear medicine can be a game-changer in this context [4–9].

Comprehending the pathophysiology encompassing CA is essential to explaining imaging findings. Extracellular amyloid infiltration leads to remodeling of the extracellular matrix and expansion of extracellular volume, rarefaction of capillary density, edema, and changes in cardiomyocyte volume leading to thickening and stiffness of ventricular walls. In the process of time, high ventricular filling pressure causes ventricular dysfunction. Atrial wall infiltration may be present as well and induces functional and electrical changes [10].

Typically, echocardiography and CMR can detect CA in the late stages of the disease. Indirect targets for imaging findings are interstitial expansion (increased ventricular and atrial wall thickness, late gadolinium enhancement, and abnormal gadolinium kinetic), inflammation, and edema (increased T2 signal on CMR). However, CMR can also direct imaging of amyloid fibrils using T1 maps. Moreover, nuclear technics can image indirect targets as increased tissue calcium (scintigraphy with bone-seeking tracers and 18F sodium fluoride PET) as well as the amyloid fibrils themselves. Amyloid-binding PET tracers, such as C-11-PIB, F-18-florbetapir, and F-18-florbetaben, are structurally like thioflavin-T and are supposed to bind to the b-pleated sheet structure of the amyloid fibril [4, 9, 10].

19.3 Cardiac SPECT in the Diagnosis of Amyloidosis

The potential use of ^{99m}Tc-labeled bone-seeking tracers to diagnose CA has been investigated for many years. Initial studies revealed high-diagnostic accuracy for

CA. Even so, other authors described different results and the interest in this field of work had diminished [11, 12]. Just recently, Perugini et al. demonstrated greater binding avidity of 3.3-diphosphono-1,2-propanodicarboxylic acid (^{99m}Tc-DPD) to ATTR rather than AL which has renewed expectations regarding the noninvasive diagnosis of ATTR CA [13].

Lately, ^{99m}Tc-labeled myocardial bone-avid radiotracer has emerged as an essential tool for the diagnosis of ATTR CA. Technetium-99m pyrophosphate (^{99m}Tc-PYP), ^{99m}Tc-DPD, and hydroxymethylene diphosphonate (^{99m}Tc-HMPD) have all shown high accuracy for imaging cardiac TTR amyloid [7].

The precise molecular mechanism behind differential uptake in ATTR and AL CA is not well known, but has been postulated that it might be related to a higher calcium content, i.e., microcalcifications in TTR amyloid fibrils. The phosphate domains in those tracers are supposed to bind to calcium in transthyretin fibrils [14–16]. It is important to point out that in the past years those tracers were primarily used to detect myocardial necrosis. Animal models experiments have revealed binding sites to bone-avid radiotracers such as microcalcifications, calcium deposits, and intracellular calcium PYP. Amyloid fibrils are mainly formed by the precursor protein, heparan sulfate proteoglycan, and a calcium-dependent P-component that holds fibrils together. Pepys et al. [14] suggest that the P-component could bind to amyloid fibrils via a calcium-mediated mechanism elucidating the process underlying bone-seeking tracers uptake in CA as well. Afterward, Stats et al. [16] showed microcalcifications in endomyocardial biopsies samples. ATTR fibrils usually have a higher concentration of microcalcifications than AL, even so, in a few cases of AL CA the amount of microcalcifications is comparable. This finding suggests a pathophysiological basis to explain why patients with AL CA may have positive scans and reassure the importance of always excluding plasma cell gammopathies.

^{99m}Tc-PYP is the only agent approved by the Food and Drug Administration (FDA) to be used in ATTR CA diagnosis in the USA and is the most used in Brazil as well. ^{9m}Tc-DPD and ^{99m}Tc-HMPD are currently the most used in Europe and other countries. On this basis, studies comparing the accuracy of those agents are scant in literature, but it seems they perform equally on ATTR CA diagnosis. As well, grading systems and imaging protocols may differ in different countries [17, 18]. Of note, ^{99m}Tc methylene diphosphonate (^{99m}Tc-MDP) is currently used for bone scintigraphy, but not recommended for ATTR CA diagnosis because of its low sensitivity [13].

19.4 Imaging Protocols

Nowadays, ^{99m}Tc-PYP and ^{99m}Tc-DPD are the most widely used radiotracers for the diagnosis and prognosis of ATTR CA. Still, data about technical aspects regarding how to image and interpret scans are not consistent in the published literature and consequently not in clinical practice as well. Lately, Practice Points and Consensus have been published in order to guide good practice [18–21].

19.5 ^{99m}Tc-DPD Imaging Protocol and Interpretation

The only formal contraindication to the test is pregnancy, which is very unlikely in daily practice since amyloidosis is a disease of older patients and no specific test preparation is required. These recommendations apply to all three radiotracers (^{99m}Tc-PYP, ^{99m}Tc-DPD, and ^{99m}Tc-HMPD).

An activity dose of 10–20 mCi (370–740 MBq) of ^{99m}Tc-DPD is administered intravenously. After 2 or 3 h of injection, a whole-body scan in the anterior and posterior views and chest anterior and lateral views are acquired followed by chest/cardiac single photon emission computed tomography (SPECT) imaging. Whenever possible, a hybrid acquisition using SPECT/CT is advisable.

A visual or semiquantitative analysis can be done at 3 h of planar imaging. Radiotracer uptake into the bones (rib) is compared to heart uptake and scored as previously described by Perugini et al. [13]: grade 0 (no heart uptake and normal rib uptake), grade 1 (heart uptake is mild and less than rib uptake), grade 2 (heart uptake is moderate and equal to rib uptake), and grade 3 (heart uptake is high and greater than rib uptake with mild or absent rib uptake). Heart uptake must be confirmed in SPECT or SPECT/CT images. Scans showing visual scores of greater than or equal to 2, i.e., 2 or 3 on SPECT images, are classified as positive and suggestive of ATTR CA. The final diagnosis encompasses the exclusion of monoclonal gammopathy.

As the visual analysis is hugely dependent on observer proficiency, it performed poorly when estimating the degree of amyloid burden [22]. In order to increase the diagnostic accuracy of the test, Rapezzi et al. [23] described a quantitative analysis that is performed by calculating the ratio between radiotracer uptake in the heart and radiotracer uptake in the body: heart/whole-body ratio (H/WB). This method has the advantage of quantitation of radiotracer retention, but requires a long time, since a late whole-body imaging must be performed, and its value is not well-established with SPECT. Interestingly, different from ^{99m}Tc-PYP scintigraphy, ^{99m}Tc-DPD might have a role in detecting extracardiac AL when no heart uptake is revealed [24].

19.6 ^{99m}Tc-PYP Imaging Protocol and Interpretation

^{99m}Tc-PYP has been used for different purposes in clinical practice: bone scintigraphy, blood pool imaging for gastrointestinal bleeding, and radionuclide ventriculography, and in the past for identification of myocardial infarction.

An activity dose of 10–20 mCi (370–740 MBq) of ^{99m}Tc-PYP is administered intravenously. After 2–3 h of injection, anterior and lateral chest planar imaging are acquired, followed by a Cardiac SPECT imaging. Whenever possible, a hybrid acquisition using SPECT/CT is advisable.

A visual or semiquantitative analysis can be obtained using planar imaging. Radiotracer uptake into the bones (rib) is compared to heart uptake and rated as previously described by Perugini et al.: grade 0 (no heart uptake and normal rib

uptake), grade 1 (heart uptake less than rib uptake), grade 2 (heart uptake equal to rib uptake), and grade 3 (greater than rib uptake with mild/absent rib uptake). Heart uptake must be confirmed in SPECT or SPECT/CT images. Scans showing visual scores of greater than or equal to 2, i.e., 2 or 3 on planar and SPECT images, are classified as positive and suggestive of ATTR CA, in case of excluding monoclonal gammopathy.

^{99m}Tc-PYP also allows quantitative analysis. Bokhari et al. [25] defined a simpler technique based on drawing a circular region of interest (ROI) over the heart on the anterior chest planar imaging and mirroring this ROI over the contralateral chest to adjust for background and ribs. Heart -to-contralateral lung uptake ratio (H/CL) is calculated as a ratio-of-heart ROI mean counts to contralateral chest ROI mean counts. H/CL >1.5 at 1 h-imaging and H/CL >1.3 at 3-h imaging is highly accurate to diagnose ATTR CA. Hence, some caution is needed when drawing the ROI, such as size adjustment to maximize coverage of the heart without including adjacent lung and avoiding sternal, ribs, and right ventricle areas in order to obtain reliable ratios. Even so, H/CL may be falsely low or high in situations like prior myocardial infarction and pleural effusion.

Some technical and pathophysiological considerations regarding bone-seeking scintigraphy must be highlighted.

Planar imaging alone is limited in spatial resolution when compared to SPECT or SPECT/CT: myocardial uptake cannot be differentiated from blood pool uptake, overlying rib uptake may add counts to the region of the heart, and attenuation correction is not feasible. SPECT overcomes these limitations and should always be performed [26]. Indeed, Régis et al. [27] showed that visual analysis on SPECT imaging has led to less scans interpreted as equivocal when compared to quantitative analysis (H/CL).

Hutt et al. [28] have demonstrated that myocardial and bone uptake over time is distinct. As the peak of myocardial counts on planar images occurs after 1 of injection of ^{99m}Tc-DPD followed by a progressive decline over time, bone counts increase gradually and peak after 2–3 h. Therefore, 1-hour imaging is more sensitive, and 3-h imaging is more specific for ATTR CA diagnosis. Similar kinetics is observed with the other radiotracers. It is important to highlight that a 1-h imaging protocol is equivalent to 3-h protocol since SPECT/CT images are incorporated which impacts positively on patient comfort and laboratory outthought [29, 30].

19.7 Critical Points Concerning ^{99m}Technetium-Labeled Cardiac Scintigraphy for Suspected Amyloidosis

The initial description of a semiquantitative visual assessment of planar images based on comparing uptake between the bone (rib) and myocardium was proposed by Perugini et al. [13]. The results showed that a grade 2 or 3 was 100% sensitive at detecting ATTR cardiac amyloidosis and 100% specificity at differentiating ATTR

from AL or unaffected controls. The utility of such a method to distinguish AL and ATTR is crucial in the workup of amyloidosis patients [31], but some critical aspects need to be highlighted to avoid mistakes:

1. Cardiac uptake with bone tracers is not specific for ATTR-CA. In a large cohort of patients with AL CA, 99mTc-DPD scintigraphy showed cardiac uptake in 40%, including grade 2–3 in 10% of all patients (25% of those with cardiac 99mTc-DPD uptake) [32].
2. The reason for cardiac DPD/PYP/HMDP preferentially in ATTR-CA is not determined. Despite some suggestions relating cardiac microcalcifications as a possible explanation [16], this does not explain why 18F-NaF PET have a relatively low sensitivity with high specificity [33]. 18F-NaF PET/MRI may have a better diagnostic performance when semiquantification is used [34].
3. To avoid falsely classifying patients with AL-CA as ATTR-CA, it is always required evaluation for AL amyloidosis by serum FLCs, serum, and urine immunofixation in all patients undergoing 99mTc-PYP/DPD/HMDP scans for cardiac amyloidosis [18]. Incorrect diagnosis leads to inappropriate therapy and worse patient outcomes. The imaging physician must clearly communicate the need to correlate imaging and laboratory findings to achieve correct diagnosis.
4. A negative scan does not exclude ATTR-CA. False negative is early disease with mild infiltration. Also important is that certain specific genetic variants such as Phe64Leu and Val30Met are not positive in bone tracer scans [35, 36]. Even patients with severe myocardial infiltration may demonstrate a false negative Tc-PYP scans as recently showed by Emory University group in patients with Val122Ile ATTR-CA [36]. This emphasizes the need for genetic testing and endomyocardial biopsy when there are inconsistent results in the clinical and laboratory evaluation.
5. Planar imaging and H/CL ratio alone are insufficient for diagnosis of ATTR cardiac amyloidosis. SPECT imaging is necessary to demonstrate myocardial uptake of 99mTc-PYP/DPD/HMDP [18]. False positive results are commonly derived from blood pool uptake. Recently, expert consensus recommendations for multimodality imaging in cardiac amyloidosis were revised and the recommended time between injection of 99mTc-PYP and scan 2- or 3-h imaging with 1-h imaging being optional.
6. Another important revision is that SPECT imaging is required in all studies (irrespective of time between injection and scan) to directly visualize tracer uptake in the myocardium [18, 37].
7. Recent data now suggest that the use of cadmium zinc telluride (CZT) SPECT for 99mTc-PYP/DPD/HMDP imaging is an alternative for planar imaging. New studies are needed to establish if better quantification can be achieved with CZT SPECT [37, 38].
8. New methods to improve the amyloid burden quantification in the myocardial are crucially needed. Since the introduction of approved therapies for transthyretin cardiac amyloidosis, there is a need to evaluate the direct effect of these agents in stopping or reversing the amyloid deposition. 99mTc-pyrophosphate

cardiac imaging using a CZT SPECT/CT scanner generated indexes such as SUVmax and SUVmean, which can provide absolute quantitation of 99mTc-pyrophosphate uptake [39].

Illustrative Cases

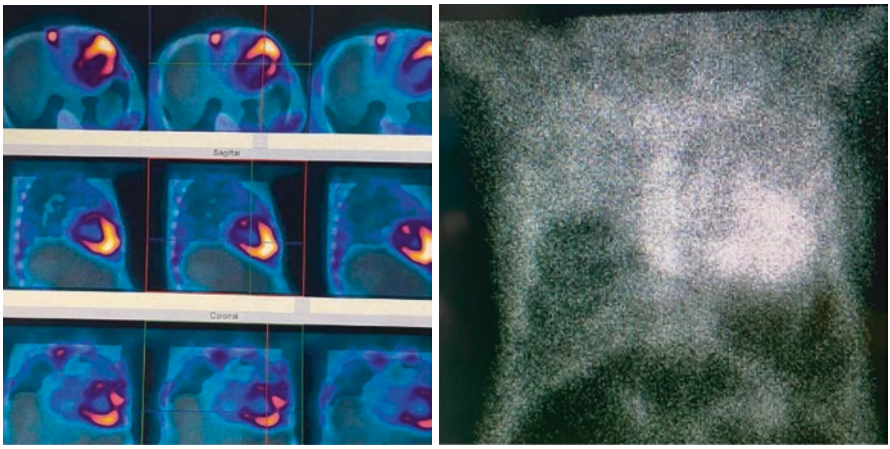

Case 1: Male patient with 74 years presenting with severe right heart failure demonstrating moderate ascites without portal hypertension. Transthoracic echocardiogram showed significant left ventricular hypertrophy (15 mm) and preserved ejection fraction. 99mTc-pyrophosphate planar imaging (right) demonstrated cardiac uptake higher than observed in ribs (Periguni score 3+). SPECT demonstrating diffuse uptake in myocardium. This case is a true positive of cardiac amyloidosis. After the adequate exclusion of monoclonal gammopathy, a diagnosis of ATTR-cardiac amyloidosis can be correctly made.

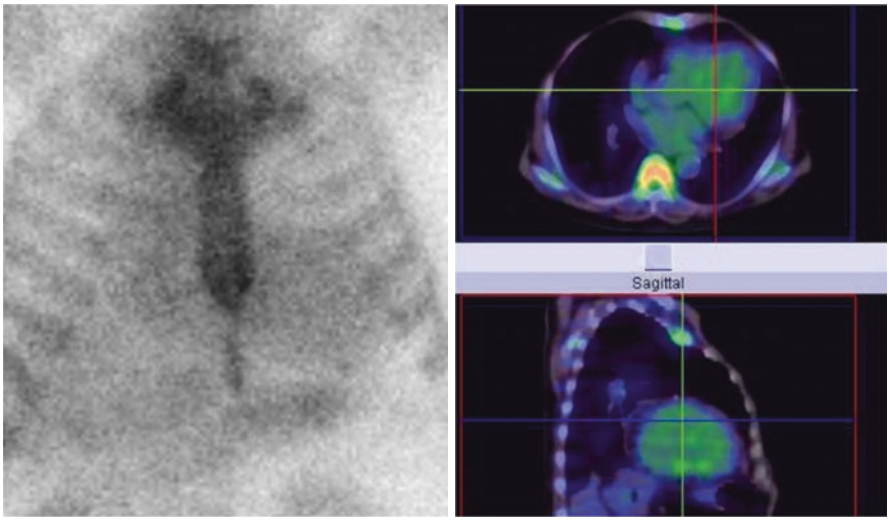

Case 2: Female patient with 52 years presenting with dyspnea and fatigue. Transthoracic echocardiogram showed borderline left ventricular hypertrophy (12 mm) and preserved ejection fraction. 99mTc-pyrophosphate planar imaging (left) demonstrated cardiac uptake like the observed in ribs (Periguni score 2+). SPECT demonstrating blood pool uptake and no accumulation in the myocardium. This case is a false positive for cardiac amyloidosis.

19.8 False-Positive and False-Negative Scenarios in Bone-Seeking Scintigraphy [2–4, 31]

As mentioned before, bone-seeking scintigraphy is a highly accurate method to diagnose ATTR CA. However, some peculiar scenarios should always be considered.

Listed below are the major causes of false-positive and false-negative results observed on bone-seeking cardiac scintigraphy.

Possible False-Positives of Scintigraphy for Detecting ATTR CA:

1. AL CA is the most common and important cause of misdiagnosis. Most clinicians are not familiar with the fact that nearly 20% of scans can be positive in patients with AL CA or the screening to rule out is not or incompletely performed.
2. Blood pool uptake in planar images. Despite being not recommended, some labs still use solely planar images to diagnose CA and a blood pool can be interpreted as a positive scan. Cardiac uptake on planar images must always be confirmed in SPECT or SPECT/CT images.
3. Rib fractures, valvular, and annular calcifications. In this case, these structures may overlay the heart, thereby affecting H/CL results. Currently, H/CL alone is not recommended to diagnose CA.
4. Myocardial infarction (acute or subacute). Focal uptake can be present, and scintigraphy should not be used to diagnose CA in this early phase (<4 months).
5. Hydroxychloroquine cardiotoxicity requires histological confirmation.
6. Rare forms of CA like hereditary apolipoprotein A1.

Possible False Negatives of Scintigraphy for Detecting ATTR CA:

1. Early-stage disease. The myocardial infiltration can be minimal and not detectable.
2. Some pathogenic TTR mutations. Phe64Leu, Val30Met, Se77Tyr, Glu61Ala. Echocardiogram or CMR may show typical findings, but scintigraphy is negative. Endomyocardial biopsy, genetic testing, and sometimes PET/CT scans can be helpful.
3. Myocardial infarction (chronic phase). Amyloid deposition and thus radiotracer uptake will be present only in viable tissue. In the context of an extensive cardiac scar, the degree of radiotracer uptake on planar imaging may be mild. However, this can be reconciled using SPECT imaging.
4. Delayed or premature acquisition protocol. Labs should always perform scans according to guidelines.

19.9 Role of Cardiac SPECT in the Context of Multimodality Imaging for Cardiac Amyloidosis Diagnosis

Currently, the most applied noninvasive methods to diagnostic and prognostic purposes in CA are echocardiography, CMR, and scintigraphy with bone-seeking tracers [1, 9, 10, 18].

Echocardiography is the first-line method used to assess CA because it is widely available and of low cost. Typical echocardiographic findings in CA include biventricular wall thickening, increased ventricular mass, normal to small ventricular size, bi-atrial enlargement, diastolic biventricular dysfunction, and preserved ejection fraction (EF). In CA, left ventricular (LV) EF (LVEF) is preserved until late to end-stage disease, but longitudinal LV contraction is impaired early in the disease [40]. A regional pattern of strain with severe impairment at the mid and basal segments and relative apical sparing of longitudinal strain is sensitive (93%) and specific (82%) to differentiate CA from other causes of LV hypertrophy [41] and abnormal global longitudinal strain is an independent predictor of poor survival in both forms of CA [40, 42, 43]. Right ventricular (RV) involvement is most commonly observed in ATTR CA [9]. Unexplained RV thickening and impaired longitudinal strain can be a red flag for initial disease and worse prognosis [44, 45]. RV dilatation in end-stage disease also portends a worse prognosis [46].

CMR provides better spatial resolution than echocardiography, allowing improved morphological and functional analysis. Besides, it is exceptional in tissue characterization. Subendocardial or transmural late gadolinium enhancement (LGE) is the most typical pattern [47, 48]. Sensitivity and specificity are 86% and 92%, respectively [49]. LGE is highly prevalent (100% RV and 96% LV) and more extensive in ATTR, but does not distinguish between CA forms. Nonetheless, it is a strong predictor of mortality in both forms of CA [50]. A limitation of LGE is that it is not simply quantifiable, which makes it inaccurate for tracking changes over time and monitoring treatment. The newer quantitative technique of T1 mapping can overcome this limitation and potentially detect amyloid infiltration earlier in the disease process than LGE and follow changes over time as well monitoring treatment response [50–53].

The only imaging modality that can accurately diagnose ATTR CA without the need for invasive endomyocardial biopsy is nuclear scintigraphy using bone-seeking radiotracers [7, 17].

Perugini et al. [13] have first described that ^{99m}Tc-DPD scintigraphy is well accurate for diagnosis and differentiates ATTR from AL in patients with documented CA (LV thickness >12 mm identified in echocardiography). The presently known as Perugini visual score was used to identify patients with ATTR CA. Some years later, Hutt et al. [54] confirmed Perugini's findings and also demonstrated that stratification by Perugini grade of positivity had no prognostic value. Later on, other authors have confirmed scintigraphy as an accurate diagnostic method even when other types of bone-seeking tracers were used [25, 55].

Rapezzi et al. [23] validated ^{99m}Tc-DPD scintigraphy as an early diagnostic method, even before the appearance of echocardiography abnormalities and established ^{99}Tc-DPD myocardial uptake (H/WB) as a prognostic determinant of cardiac outcomes either alone or in combination with LV wall thickness.

In a multicentric study, Castano et al. [56] pointed out that semiquantitative data obtained from ^{99m}Tc-PYP scintigraphy were associated with worse survival and consequently poor prognosis among patients with ATTR CA; and, that the test could be reproducibly performed at multiple sites with high accuracy. Sperry et al. [57] showed a pattern similar to apical sparing in scintigraphy too and also associated with prognosis. Furthermore, absolute quantification using SPECT/CT might be valuable for improving the diagnosis and prognosis of ATTR CA [58].

Quite a few studies have confirmed scintigraphy as an excellent method for early diagnosis [23, 59]. However, the scintigraphy role in following up is still uncertain [60]. In this context, data from CMR studies are very promising [61].

Gillmore et al. [7] have revolutionized clinical practice by proposing that ATTR CA could be noninvasively diagnosed using bone-seeking scintigraphy. In this multicenter study involving 1217 patients with suspected CA, any myocardial radiotracer uptake (grade 1, 2 or 3) was >99% sensitive and 86% specific for detecting ATTR CA, with false-positive cases being attributed to AL CA. Indeed, 30% of patients with CA AL may have positive scans. Grades 2 or 3 of myocardial radiotracer uptake and the absence of monoclonal gammopathies in serum or urine had a specificity and positive predictive value of 100% to detect ATTR CA. Of note, these results were obtained in a population of patients with a high pretest probability of CA: symptoms of heart failure and echocardiogram or CMR consistent with CA. More studies are needed to confirm if these findings can be used in the general population without all these characteristics of this population.

19.10 Myocardial Innervation Evaluation in CA

Cardiac dysautonomia is common in both types of CA (ATTR and AL types) [62]. This is due to amyloid infiltration into the myocardial and conduction tissue, resulting in conduction and rhythm disorders. Amyloid deposits impair the function of sympathetic nerve endings. Disturbance of myocardial sympathetic innervations may play an important role in the remodeling process. Imaging of myocardial innervation in patients with amyloidosis has been mainly focused on visualizing the effects of amyloidosis on the sympathetic nerve system [62, 63].

Conventional nuclear imaging by means of 123-Iodine-metaiodobenzylguanidine (^{123}I-mIBG) is the most widely used modality for this indication [62]. It is a chemical modified analogue of norepinephrine that can detect myocardial innervation changes [64]. ^{123}I-mIBG cardiac scintigraphy is well-established in patients with heart failure [65] and plays an important role in evaluation of sympathetic innervation in CA [18, 62].

^{123}I-mIBG is stored in vesicles in the sympathetic nerve terminals and is not catabolized like norepinephrine [64]. Cardiac ^{123}I-mIBG uptake can be evaluated using both planar and tomographic imaging, thereby providing insight into global and regional sympathetic innervation. Standardly assessed imaging parameters are the heart-to-mediastinum ratio (HMR) and washout rate (WR), usually derived from planar images. Decreased HMR 3–4 h after ^{123}I-mIBG injection (late HMR) and increased WR indicate cardiac sympathetic denervation and are associated with poor prognosis [62, 64]. SPECT provides additional information and has advantages for evaluating abnormalities in regional distribution in the myocardium [65]. ^{123}I-mIBG is mainly useful in patients with ATTRv CA and ATTRw CA, not in AA and AL amyloidosis [62]. The potential role of PET for cardiac sympathetic innervation in amyloidosis has not yet been identified [62, 66].

In a review paper that included 16 studies on this subject [62], the results were summarized and divided into three main topics: the imaging of cardiac innervation itself, the implications of this imaging method, and the relation with other nuclear medicine imaging techniques in CA. In relation to the imaging of cardiac innervation, ATTRv type amyloidosis patients are studied most extensively, showing the most pronounced reduced late HMR. Also, AL type amyloidosis patients tend to have decreased late HMR compared to healthy control subjects; however, to a lesser extent compared to both ATTRv CA and ATTRw CA type patients [62, 67–69]. In a study with 61 CA patients (39 AL, 11 AA, 11 ATTR), late ^{123}I-mIBG HMR was lower and WR was higher in patients with echocardiographic signs of amyloidosis. In ATTR CA patients without echocardiographic signs of amyloidosis, HMR was lower than in patients with the other CA types (2.0 ± 0.59 vs. 2.9 ± 0.50, $p = 0.007$). Then, ^{123}I-mIBG scintigraphy could detect cardiac denervation in ATTR CA patients before signs of amyloidosis are evident on echocardiography [69]. However, due to the large overlap of late HMR ranges in ATTR and AL type amyloidosis patients, ^{123}I-mIBG scintigraphy is not capable of discriminating between these amyloidosis subtypes [69].

Mean late HMR differs substantially between the different publications [62]. This variability is mainly due to non-homogeneity in^{123}I-mIBG imaging acquisition. HMR varies between different gamma camera systems (venders), but more importantly between the application of low energy and medium energy collimators [62, 64]. Generally, HMR is higher on images acquired with medium energy collimators compared to images acquired with low energy collimator [70]. Based on these differences in HMR, cutoff values for the different collimators are proposed, as well as conversion algorithms. Additional SPECT scanning may be of value in the evaluation of regional cardiac sympathetic innervation abnormalities. Most patients (both AL and ATTR type amyloidosis) with low HMR show reduced tracer accumulation in the infero-postero-lateral segments [69]. Unfortunately, this may not be considered as a characteristic finding in amyloidosis patients, since a defect in ^{123}I-mIBG accumulation in the inferior myocardial wall is also reported in healthy control subjects [71]. This is considered because of physiological ^{123}I-mIBG accumulation in the liver overprotecting the infero-posterior myocardial wall [18, 62, 64, 71].

Concerning the clinical implications of this imaging technique, in patients with heart failure, the ADMIRE-HF demonstrated that reduced late HMR is associated with an increased risk of developing ventricular arrhythmia and is associated with poor survival [72]. In fact, reduced late HMR is a stronger prognostic factor than LVEF for developing severe adverse cardiac events in patients with ischemic heart disease [65]. In amyloidosis patients with impaired cardiac sympathetic innervation, decreased survival rates are also established [73]. Late HMR was identified as an independent prognostic factor for 5-year all-cause mortality, with a 42% mortality rate for those patients with late HMR <1.60, compared to only 7% in patients with late HMR ≥1.60 (hazard ratio 7.2, $P < 0.001$) [73].

In the AL type population, very little is known about the consequences of reduced late HMR. Follow-up of the available studies in this population is too limited to identify arrhythmogenic consequences of impaired cardiac sympathetic innervation [62, 69]. Data on the contribution of reduced late HMR to cardiovascular outcome measurements in patients with ATTR CA amyloidosis seem to be incomplete. Moreover, the actual incidence of ventricular arrhythmia, sudden cardiac death, or appropriate implantable cardioverter-defibrillator (ICD) shocks in amyloidosis patients with impaired cardiac sympathetic innervation is not fully elucidated. Therefore, the question whether amyloidosis patients will benefit from prophylactic ICD remains unanswered [62].

In comparison to other nuclear medicine imaging techniques, cardiac ^{123}I-mIBG scintigraphy cannot discriminate between ATTR CA and AL CA as bone tracer scintigraphy does. Moreover, since both ATTRw and ATTRv patients show decreased late HMR, this exam alone could not differentiate between autonomic neuropathy and cardiomyopathy. Bone tracer accumulation predominantly occurs in ATTRw CA patients, probably as a result of the underlying cardiomyopathy. On the contrary, patients with ATTRv type amyloidosis without cardiomyopathy tend to show no myocardial bone tracer accumulation and normal biomarkers (N-terminus pro-brain natriuretic peptide, and troponin-T) [62]. Within these patients, late HMR is generally lower in the subgroup of patients with other symptoms of polyneuropathy [74]. Future studies should focus on the possible additive value of bone scintigraphy in relation to ^{123}I-mIBG scintigraphy in getting a better understanding of the complementary contribution of neuropathy and cardiomyopathy to each other in ATTR type amyloidosis patients [62].

19.11 Diagnostic Algorithms of Cardiac Amyloidosis

Guidelines and consensus support a non-biopsy diagnosis of ATTR CA using ^{99m}Tc-PYP/DPD/HMDP scintigraphy. Gillmore et al. [7] showed that scintigraphy is highly sensitive, but not so specific for ATTR CA diagnosis and most false-positive scans were attributed to AL CA. Ruling out monoclonal gammopathies is essential. There is no consensus if laboratory tests to exclude AL should be done before or after scintigraphy is performed. It is important to point out that up to 40% of patients

with ATTR CA can have a monoclonal gammopathy of unknown significance (MGUS) and an endomyocardial biopsy is necessary to confirm ATTR CA [75]. After ATTR CA is confirmed, TTR gene sequencing and genetic counseling for relatives are advised.

Some diagnostic algorithms of CA have been proposed [3, 6, 18]. Indeed, they are quite similar. The most important difference is regarding when tests to exclude gammopathies should be done, i.e., before scintigraphy or after.

19.12 Quantitative Studies to Assess Disease Activity and Response to Therapy

^{99m}Tc-labeled bone-seeking tracers cardiac scintigraphy to diagnose and prognosis ATTR CA is not an absolute quantitative method since visual and semiquantitative analysis compare cardiac radiotracer uptake to other tissues.

Perugini et al. [13] demonstrated that visual analyses accurately discriminate patients with ATTR CA from those with AL CA and controls. However, the Perugini score was not a predictor of prognosis [54]. Of note, ATTR is a systemic disease and abnormal protein deposits can be present in extracardiac sites. The main criterion used to differentiate grade 2 from grade 3 of the Perugini score is the reduction in bone uptake. So, in some cases, grade 3 might be related to extracardiac uptake rather than true greater cardiac uptake. This hypothesis might explain why the visual score has not been proven to be useful in risk stratification [58].

In order to improve the measurement of cardiac uptake of ^{99m}Tc-labeled bone-seeking tracers, semiquantitative ratios, namely, H/CL and H/WB, have been proposed. Yet, this technique still relies on extracardiac sites as comparators. Castano et al. [56] described that H/CL has prognostic significance, but the cutoff value for diagnosis and worse prognosis is narrow. Also, the role of H/WB is still uncertain [76]. Accordingly, semiquantitative assessment did improve diagnosis but not prognosis.

As postulated, the exact mechanism behind bone-seeking tracer uptake in ATTR CA is not recognized, but it's reasonable to assume that a greater cardiac amyloid deposition may be associated with more scan uptake and consequently worse prognosis and that changes in amyloid burden could be assessed by changes in radiotracer uptake. Planar imaging carries important limitations and SPECT is strongly recommended to improve the diagnostic performance of scintigraphy. Recently, a lot of effort has been made to develop SPECT-based quantitative techniques to evaluate burden amyloid as well as response to novel therapies [58].

At the present time, absolute quantitation of myocardial uptake can be assessed by SPECT. Quantitative SPECT images can be reconstructed using proper commercially available software, CT-based attenuation correction, scatter correction, and iterative reconstruction technique. Comparable with PET, the images represent parametric maps of radiopharmaceutical distribution with units of kBq/mL

standardized to the time of injection and can be corrected for injected dose and volume of distribution to give standard uptake value (SUV). Cardiac metabolic activity (CMA) and cardiac metabolic volume (CMV) also can be used to assess amyloid burden [50].

Ramsay et al. [77] demonstrated that quantitative HDP SPECT/CT can discriminate between individuals with cardiac ATTR from the population without this disease (p = 0,002). The SUV maximum (SUVmax) was sufficiently similar between individuals without cardiac ATTR that a 99% reference interval for HDP uptake could be calculated, providing an upper limit cut point of SUVmax 1.2. Individuals with cardiac ATTR had SUVmax well above. Still, its role in disease management warrants further assessment.

In a single-center, retrospective analysis of ^{99m}Tc-DPD scans, Scully et al. [78] showed that SPECT/CT quantification is possible and outperforms planar quantification techniques. Moreover, SUV retention index differentiates Perugini grade 2 or 3 and may be an important tool to monitor response to therapy.

Miller et al. [79] assessed the diagnostic accuracy and clinical significance of ^{99m}Tc-PYP quantitation. Radiotracer activity in the myocardium was calculated using cardiac pyrophosphate activity (CPA) and volume of involvement (VOI) activity. CPA had the highest diagnostic accuracy (AUC 0.996, 95% CI 0.987–1.00) and was significantly higher compared to the Perugini score (AUC 0.952, P = 0.016). Quantitative assessment of myocardial radiotracer activity with CPA or VOI has high diagnostic accuracy for ATTR-CM. Both measures are potential noninvasive markers to follow the progression of disease or response to therapy.

Dorbala et al. [39] were pioneers in demonstrating that absolute quantification is possible to be done using ^{99m}Tc-PYP-Cadmium-Zinc-Telluride-Based SPECT/CT.

19.13 Myocardial Blood Flow Evaluation in CA

Coronary microvascular dysfunction (CMD) can result from structural and functional abnormalities at the intramural and small coronary vessel level affecting coronary blood flow autoregulation and consequently leading to impaired coronary flow reserve (CFR) [80]. Endothelial and CMD often coexist with epicardial coronary artery disease (CAD), but are also commonly seen in patients with various forms of heart disease, including CA [18, 80–82].

Interstitial and perivascular amyloid deposits may compress coronary microvessels, thereby increasing coronary microvascular resistance. Increased LV mass may reduce capillary density and decrease diastolic perfusion from high LV filling pressures. Autonomic dysfunction may also result in vasomotor dysfunction [80]. Angina without epicardial CAD has been well-described in patients with amyloidosis [83]. Myocardial perfusion abnormalities can be detected in patients with AL and ATTR CA and may precede the clinical diagnosis of CA [83].

Dorbala et al. [81] studied 31 patients, including 21 with definite CA without epicardial CAD and 10 patients with hypertensive left ventricular hypertrophy (LVH). All of them underwent rest and vasodilator stress N-13 ammonia PET and 2D echocardiography. Global LV myocardial blood flow (MBF) was quantified at rest and during peak hyperaemia, and CFR was computed (peak stress MBF / rest MBF) adjusting for rest rate pressure product. Compared to the LVH group, the amyloid group showed lower rest MBF (0.59 ± 0.15 vs. 0.88 ± 0.23 mL/g/min, $P = 0.004$), stress MBF (0.85 ± 0.29 vs. 1.85 ± 0.45 vs. mL/min/g, $P < 0.0001$), CFR (1.19 ± 0.38 vs. 2.23 ± 0.88, $P < 0.0001$), and higher minimal coronary vascular resistance (111 ± 40 vs. 70 ± 19 mm Hg/mL/g/min, $P = 0.004$). Additionally, more than 95% of all amyloid subjects presented significantly reduced peak stress MBF (<1.3 mL/g/min). In multivariable linear regression analyses, a diagnosis of amyloidosis and increased LV mass and age were the only independent predictors of impaired coronary vasodilator function. Absolute MBF and CFR were substantially reduced in patients with CA, despite absence of epicardial CAD [81].

CMD from amyloid deposits may potentially explain a greater vulnerability of these individuals to ischemia and subclinical impairment of LV systolic function [80]. Myocardial ischemia from CMD may predispose some of these patients to sudden cardiac death. More studies are required to understand whether CMD improves after successful anti-amyloid therapy.

19.14 PET Tracers for Amyloid Detection and to Evaluate Disease Progression

PET is another nuclear technique that can be used to evaluate CA. Literature data about the role of this technique to assess CA are scant when compared to scintigraphy with bone-seeking tracers, but still very promising. PET imaging offers the advantage of higher spatial resolution and allows absolute quantification of amyloid burden and, therefore, changes after treatment. Two classes of PET radiotracers may be used: 18F Sodium Fluoride (^{18}F-NaF) and amyloid-binding radioactive tracers [9, 17].

19.14.1 ^{18}F-Sodium Fluoride

^{18}F-Sodium Fluoride (^{18}F-NaF) was used in the past for prostate cancer screening and has been studied more recently in CAD as a novel method to predict cardiac events. Like bone-seeking tracers used in scintigraphy,^{18}F-NaF also binds to microcalcifications, so it is reasonable to assume that it could be used to detect CA and differentiate ATTR from AL CA. Also, Castano et al. [60] demonstrated that

bone-seeking tracer scintigraphy is not currently useful to monitor response to treatment and ^{18}F-NaF could be useful in this scenario.

Morgenstern et al. [84] showed that ^{18}F-NaF is an effective PET radiotracer to image ATTR CA. Qualitative and quantitative analysis demonstrated higher uptake in ATTR CA when compared to AL CA patients and controls.

Martineau et al. [85] examined the sensitivity of ^{18}F-NaF PET to detect ATTR CA. Although the degree of myocardial uptake was significantly greater in ATTR patients compared to AL and control subjects, it was low and inferior to the blood pool leading to a modest sensitivity when qualitative and quantitative methods were used, 57% and 75% respectively. These findings were quite different from those obtained with scintigraphy [7]. Zhang et al. [86] were pioneers in comparing the sensitivity of ^{18}F-NaF PET in detecting CA to that of ^{99m}Tc-PYP. Both qualitative and quantitative analyses showed that PET sensitivity was significantly inferior to that of ^{99m}Tc-PYP. So, currently, data do not support the use of ^{18}F-NaF PET to diagnose ATTR CA.

19.14.2 Amyloid PET Tracers

Amyloid-binding radioactive tracers were originally developed to image brain beta-amyloid deposits in patients with Alzheimer's disease, but recently, some studies have demonstrated its capacity to bind to cardiac amyloid deposits and opened a new field of investigation. These tracers are structurally like thioflavin-T and bind to the beta-pleated motif of amyloid fibril irrespective of the precursor amyloid protein [9] ^{11}C-Pittsburgh Compound-B (^{11}C-PIB) and ^{18}F-labelled agents such as ^{18}F-florbetapir and ^{18}F-florbetaben have been successfully used to assess Alzheimer's disease and more recently as a new technique to diagnose CA [87].

Antoni et al. [88] demonstrated that ^{11}C-PiB can accurately differentiate controls from patients with confirmed CA. However, it was not capable of differentiating ATTR from AL CA. Later on, Rosengren et al. [89] showed that ^{11}C-PiB could also accurately distinguish AL from ATTR CA patients since quantitative methods have shown that radiotracer uptake was significantly higher in AL CA. However, the need for an onsite cyclotron for production, due to its short half-life, limits its availability and clinical use.

^{18}F-labeled amyloid imaging tracers have a longer half-life, thus, allowing their use in laboratories without a cyclotron. Initial studies using ^{18}F-Florbetapir [90, 91] have demonstrated a significant radiotracer uptake in patients with CA and no uptake in controls. Although uptake was higher in AL than in ATTR CA, it was not sufficient to discriminate AL from ATTR CA. Studies using ^{18}F-Florbetaben have demonstrated similar findings [92]. More recently, Genovesi et al. [93] demonstrated in a prospective study that ^{18}F-Florbetaben uptake over time was significantly higher in patients with AL CA than in ATTR CA allowing type differentiation.

Importantly, only amyloid-binding PET tracers can adequately image AL CA and identify systemic amyloid deposits.

Regarding the response to therapy, initial data are promising, but more studies are needed to warrant its clinical use [9].

In conclusion, further large multicenter studies would be necessary to substantiate the diagnostic accuracy of PET for the detection of CA [94].

19.15 Future Perspectives

Certainly, we have learned much about CA over the past few years. Great achievements in multimodality imaging methods have led to the noninvasive diagnosis of ATTR CA in a substantial number of patients. Meanwhile, improvements in clinical treatment, with novel drugs, brought the opportunity for better outcomes. Even so, some uncertain issues demand further investigation.

Bone-seeking tracers scintigraphy has proved to be highly accurate in the diagnosis of ATTR CA, but these data were obtained from a population with a high likelihood of disease. May we extrapolate to a less selected one? Is the method accurate for screening in patients with aortic stenosis or bilateral carpal tunnel syndrome, currently known as red flags of disease? Its utility remains unproven and ongoing studies will provide insight into this matter. In this respect, the implementation of appropriate screening programs for ATTR CA is also mandatory to increase awareness of the disease.

A better understanding of amyloidogenesis pathophysiology and differences between the phosphate-derived radiotracers with respect to diagnosis, subtyping, and prognostication of ATTR is crucial. Also, technical refinements on scan acquisition and standardization of radioisotope dose, incubation time, and analytic ROI methods are needed.

SPECT and PET/CT are promising tools for quantification and assessment of response to therapy, but more robust data are needed to define their accuracy and additive value to the care of patients with cardiac amyloidosis.

Clinical Case

A 70-year-old-male with a history of hypertension, diabetes, and dyslipidemia presented with progressive exertional dyspnea that had persisted for the previous month. Bilateral Carpal Tunnel Syndrome Operation in 2013. Patient was admitted to the cardiac care unit for acute heart failure (HF) in the New York Heart Association (NYHA) class IV. Transthoracic echocardiogram revealed bi-atrial enlargement. Normal ventricle size. Severe concentric left ventricular hypertrophy (19 mm), preserved overall systolic biventricular function (Fig. 19.1). Impaired relaxation and elevated filling pressures with restrictive mitral inflow pattern were consistent with diastolic dysfunction grade III. Mild mitral and tricuspid regurgitation were also

noticed. A pattern of apical sparing on the longitudinal strain was observed too (Fig. 19.2). A Cardiac MRI was pursued and depicted heterogeneous subendocardium late gadolinium enhancement encompassing atrium, interatrial septum, interventricular septum, and right and left ventricles consistent with infiltrative disease (Figs.19.3 and 19.4). Cardiac amyloidosis was suspected and 99mTc-PYP scintigraphy was performed. Planar images showed abnormally increased radiotracer activity in the heart (Perugini grade 3) with a calculated heart-to-contralateral ratio (H/CL) of 1.7. (Fig. 19.5) SPECT/CT images confirmed uptake throughout the myocardium and right ventricle (Figs. 19.6 and 19.7). Gamophathies were excluded. Genetic testing showed the mutation Val142Ile confirming ATTR CA.

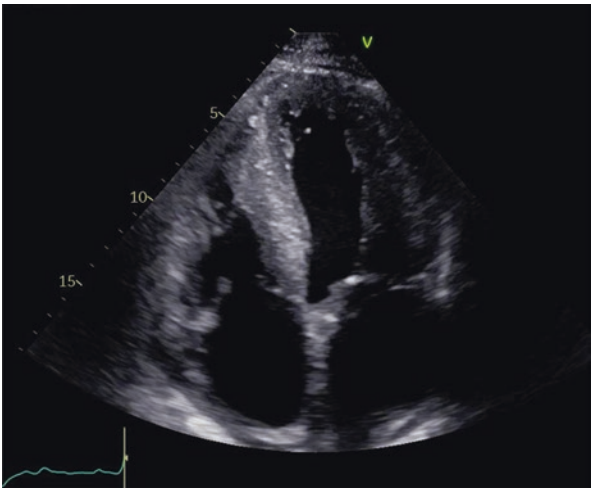

Fig. 19.1 Echocardiogram 4-chamber view (Author's personal archive)

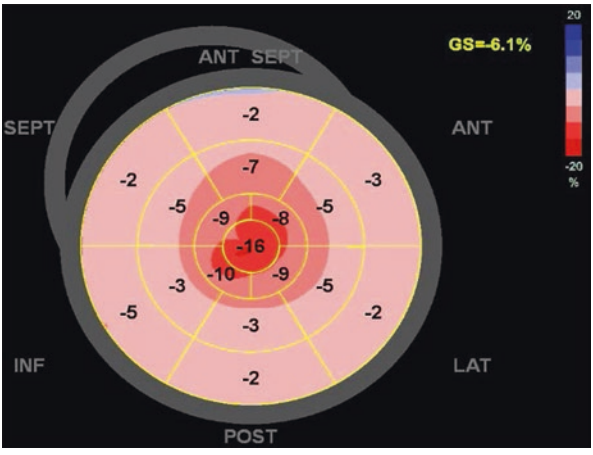

Fig. 19.2 Bull's eye strain showing preservation of apical deformity. (Author's personal archive)

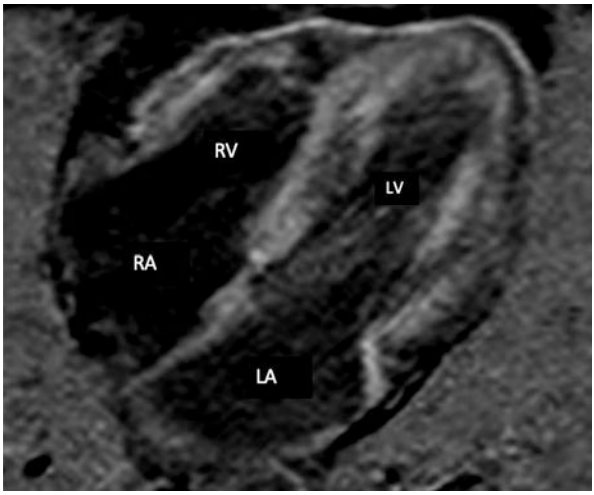

Fig. 19.3 Diffuse subendocardial LGE in 4-chamber CMR (Author's personal archive)

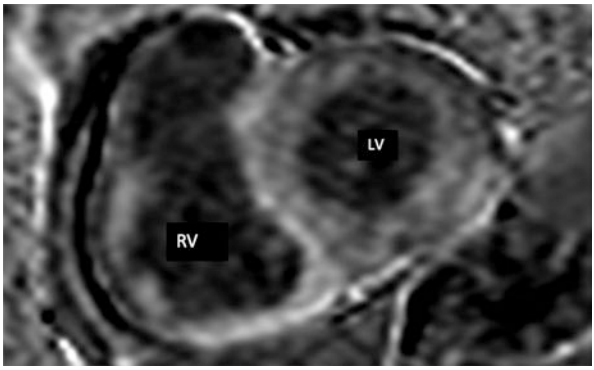

Fig. 19.4 Diffuse subendocardial LGE in short axis CMR (Author's personal archive)

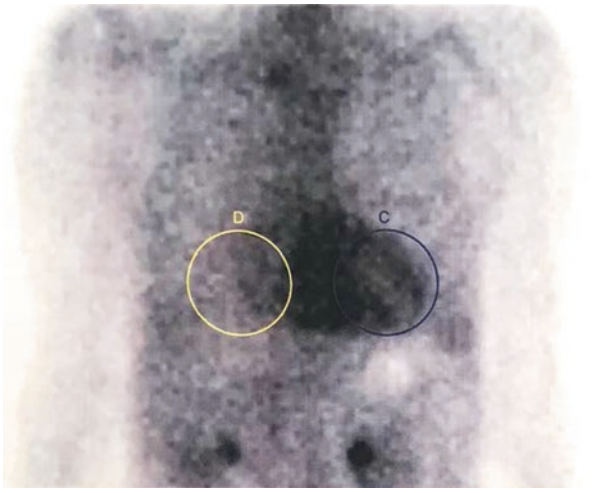

Fig. 19.5 99m-Tc-PYP anterior planar Image showing cardiac uptake greater than ribs (Perugini grade 3) and H/CL = 1.7 (Author's personal archive)

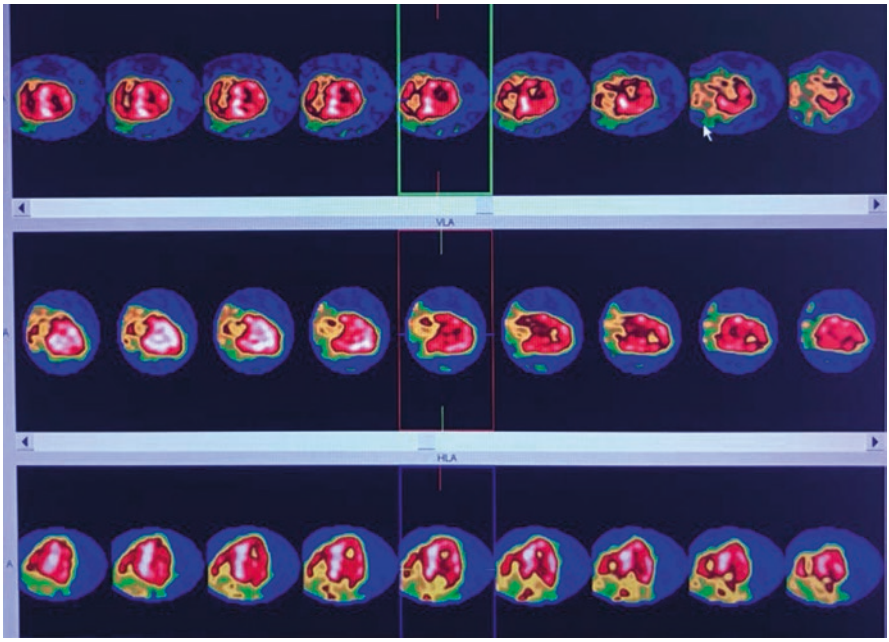

Fig. 19.6 SPECT imaging showing diffuse uptake throughout the myocardium and right ventricle (Author's personal archive)

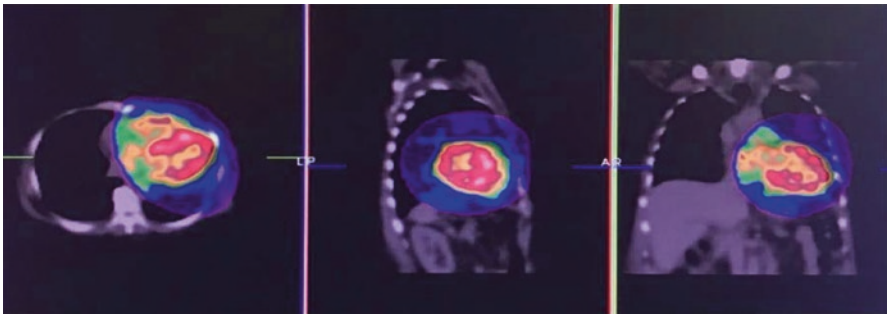

Fig. 19.7 Fused SPECT/CT imaging (Author's personal archive)

References

1. Ruberg FL, Grogan M, Hanna M, Kelly JW, Maurer MS. Transthyretin amyloid cardiomyopathy: JACC state-of-the-art review. J Am Coll Cardiol. 2019;73(22):2872–91.
2. Kittleson MM, Maurer MS, Ambardekar AV, Bullock-Palmer RP, Chang PP, Eisen HJ, et al. Cardiac amyloidosis: evolving diagnosis and management: a scientific statement from the American Heart Association. Circulation. 2020:1–16.

3. Garcia-Pavia P, Rapezzi C, Adler Y, Arad M, Basso C, Brucato A, et al. Diagnosis and treatment of cardiac amyloidosis. A position statement of the European Society of Cardiology Working Group on myocardial and pericardial diseases. Eur J Heart Fail. 2021;23(4):512–26.
4. Jurcuţ R, Onciul S, Adam R, Stan C, Coriu D, Rapezzi C, et al. Multimodality imaging in cardiac amyloidosis: a primer for cardiologists. Eur Heart J Cardiovasc Imaging. 2020;21(8):833–44.
5. Witteles RM, Bokhari S, Damy T, Elliott PM, Falk RH, Fine NM, et al. Screening for transthyretin amyloid cardiomyopathy in everyday practice. JACC Hear Fail. 2019;7(8):709–16.
6. Maurer MS, Bokhari S, Damy T, Dorbala S, Drachman BM, Fontana M, et al. Expert consensus recommendations for the suspicion and diagnosis of transthyretin cardiac amyloidosis. Circ Hear Fail. 2019;12(9):1–11.
7. Gillmore JD, Maurer MS, Falk RH, Merlini G, Damy T, Dispenzieri A, et al. Nonbiopsy diagnosis of cardiac transthyretin amyloidosis. Circulation. 2016;133(24):2404–12.
8. Li W, Uppal D, Wang YC, Xu X, Kokkinidis DG, Travin MI, et al. Nuclear imaging for the diagnosis of cardiac amyloidosis in 2021. Diagnostics. 2021;11(6):1–13.
9. Dorbala S, Cuddy S, Falk RH. How to image cardiac amyloidosis: a practical approach. JACC Cardiovasc Imaging. 2020;13(6):1368–83.
10. Fontana M, Ćorović A, Scully P, Moon JC. Myocardial amyloidosis: the exemplar interstitial disease. JACC Cardiovasc Imaging. 2019;12(11P2):2345–56.
11. Wizenberg TA, Muz J, Sohn YH, Samlowski W, Weissler AM. Value of positive myocardial technetium-99m-pyrophosphate scintigraphy in the noninvasive diagnosis of cardiac amyloidosis. Am Heart J. 1982;103(4):468–73. https://doi.org/10.1016/0002-8703(82)90331-3.
12. Gertz MA, Brown ML, Hauser MF, Kyle RA. Utility of technetium Tc 99m pyrophosphate bone scanning in cardiac amyloidosis. Arch Intern Med. 1987;147(6):1039–44.
13. Perugini E, Guidalotti PL, Salvi F, Cooke RMT, Pettinato C, Riva L, et al. Noninvasive etiologic diagnosis of cardiac amyloidosis using 99mTc-3,3-diphosphono-1,2-propanodicarboxylic acid scintigraphy. J Am Coll Cardiol [Internet]. 2005;46(6):1076–84. https://doi.org/10.1016/j.jacc.2005.05.073.
14. Pepys MB, Dyck RF, de Beer FC, Skinner M, Cohen a S. Binding of serum amyloid P-component (SAP) by amyloid fibrils. Clin Exp Immunol [Internet]. 1979;38(2):284–93. http://www.pubmedcentral.nih.gov/articlerender.fcgi?artid=1537850&tool=pmcentrez&rendertype=abstract%5Cn, http://www.ncbi.nlm.nih.gov/pmc/articles/PMC1537850/?tool=pubmed
15. Suhr OB, Lundgren E, Westermark P. One mutation, two distinct disease variants: unravelling the impact of transthyretin amyloid fibril composition. J Intern Med. 2017;281(4):337–47.
16. Stats MA, Stone JR. Varying levels of small microcalcifications and macrophages in ATTR and AL cardiac amyloidosis: implications for utilizing nuclear medicine studies to subtype amyloidosis. Cardiovasc Pathol [Internet]. 2016;25(5):413–7. https://doi.org/10.1016/j.carpath.2016.07.001.
17. Singh V, Falk R, Di Carli MF, Kijewski M, Rapezzi C, Dorbala S. State-of-the-art radionuclide imaging in cardiac transthyretin amyloidosis. J Nucl Cardiol [Internet]. 2019;26(1):158–73. https://doi.org/10.1007/s12350-018-01552-4.
18. Dorbala S, Ando Y, Bokhari S, Dispenzieri A, Falk RH, Ferrari VA, et al. ASNC/AHA/ASE/EANM/HFSA/ISA/SCMR/SNMMI expert consensus recommendations for multimodality imaging in cardiac amyloidosis: part 1 of 2—evidence base and standardized methods of imaging. J Nucl Cardiol [Internet]. 2019;26(6):2065–123. https://doi.org/10.1007/s12350-019-01760-6.
19. Sharmila D, Sabahat B, Glaudemans AWJM, Edward M, Renee B-P, et al. ASNC and EANM cardiac amyloidosis practice points (HMDP) imaging for transthyretin cardiac amyloidosis. Am Soc Nucl Cardiol; 2019
20. Imaging P, Amyloidosis C. ASNC cardiac amyloidosis practice points (www.asnc.org).
21. Dorbala S, Ando Y, Bokhari S, Dispenzieri A, Falk RH, Ferrari VA, et al. Addendum to ASNC/AHA/ASE/EANM/HFSA/ISA/SCMR/SNMMI expert consensus recommendations for multimodality imaging in cardiac amyloidosis: part 1 of 2-evidence base and standardized

methods of imaging. J Nucl Cardiol [Internet]. 2021;28(4):1769–74. https://doi.org/10.1007/s12350-020-02455-z.
22. Caobelli F, Braun M, Haaf P, Wild D, Zellweger MJ. Quantitative 99mTc-DPD SPECT/CT in patients with suspected ATTR cardiac amyloidosis: feasibility and correlation with visual scores. J Nucl Cardiol [Internet]. 2019; https://doi.org/10.1007/s12350-019-01893-8.
23. Rapezzi C, Quarta CC, Guidalotti PL, Pettinato C, Fanti S, Leone O, et al. Role of 99mTc-DPD scintigraphy in diagnosis and prognosis of hereditary transthyretin-related cardiac amyloidosis. JACC Cardiovasc Imaging [Internet]. 2011;4(6):659–70. https://doi.org/10.1016/j.jcmg.2011.03.016.
24. Sachchithanantham S, Hutt DF, Quigley AM, Hawkins P, Wechalekar AD. Role of 99mTc-DPD scintigraphy in imaging extra-cardiac light chain (AL) amyloidosis. Br J Haematol. 2018;183(3):506–9.
25. Bokhari S, Castaño A, Pozniakoff T, Deslisle S, Latif F, Maurer MS. 99mTc-pyrophosphate scintigraphy for differentiating light-chain cardiac amyloidosis from the transthyretin-related familial and senile cardiac amyloidoses. Circ Cardiovasc Imaging. 2013;6(2):195–201.
26. Asif T, Gomez J, Singh V, Doukky R, Nedeltcheva A, Malhotra S. Comparison of planar with tomographic pyrophosphate scintigraphy for transthyretin cardiac amyloidosis: perils and pitfalls. J Nucl Cardiol [Internet]. 2021;28(1):104–11. https://doi.org/10.1007/s12350-020-02328-5.
27. Régis C, Harel F, Martineau P, Grégoire J, Abikhzer G, Juneau D, et al. Tc-99m-pyrophosphate scintigraphy for the diagnosis of ATTR cardiac amyloidosis: comparison of quantitative and semi-quantitative approaches. J Nucl Cardiol. 2020;27(5):1808–15.
28. Hutt DF, Quigley AM, Page J, Hall ML, Burniston M, Gopaul D, et al. Utility and limitations of 3,3-diphosphono-1, 2-propanodicarboxylic acid scintigraphy in systemic amyloidosis. Eur Heart J Cardiovasc Imaging. 2014;15(11):1289–98.
29. Sperry BW, Burgett E, Bybee KA, McGhie AI, O'Keefe JH, Saeed IM, et al. Technetium pyrophosphate nuclear scintigraphy for cardiac amyloidosis: Imaging at 1 vs 3 hours and planar vs SPECT/CT. J Nucl Cardiol [Internet]. 2020; https://doi.org/10.1007/s12350-020-02139-8.
30. Masri A, Bukhari S, Ahmad S, Nieves R, Eisele YS, Follansbee W, et al. Efficient 1-hour Technetium-99 m pyrophosphate Imaging protocol for the diagnosis of transthyretin cardiac amyloidosis. Circ Cardiovasc Imaging. 2020;(February):1–9.
31. Hanna M, Ruberg FL, Maurer MS, Dispenzieri A, Dorbala S, Falk RH, et al. Cardiac scintigraphy with technetium-99m-labeled bone-seeking tracers for suspected amyloidosis: JACC review topic of the week. J Am Coll Cardiol. 2020;75(22):2851–62.
32. Quarta CC, Zheng J, Hutt D, Grigore SF, Manwani R, Sachchithanantham S, et al. 99mTc-DPD scintigraphy in immunoglobulin light chain (AL) cardiac amyloidosis. Eur Heart J Cardiovasc Imaging. 2021;22(11):1304–11.
33. Kim SH, Kim YS, Kim SJ. Diagnostic performance of PET for detection of cardiac amyloidosis: a systematic review and meta-analysis. J Cardiol [Internet]. 2020;76(6):618–25. https://doi.org/10.1016/j.jjcc.2020.07.003.
34. Abulizi M, Sifaoui I, Wuliya-Gariepy M, Kharoubi M, Israël JM, Emsen B, et al. 18F-sodium fluoride PET/MRI myocardial imaging in patients with suspected cardiac amyloidosis. J Nucl Cardiol. 2019;
35. Pilebro B, Suhr OB, Näslund U, Westermark P, Lindqvist P, Sundström T. 99mTc-DPD uptake reflects amyloid fibril composition in hereditary transthyretin amyloidosis. Ups J Med Sci. 2016;121(1):17–24.
36. Yadalam A, Ceballos A, Bigham T, Rim A, Yalamanchili S, Brown MT, et al. False negative cardiac scintigraphy in patients with Val122Ile transthyretin cardiac amyloidosis. J Am Coll Cardiol [Internet]. 2022;79(9):427. https://doi.org/10.1016/S0735-1097(22)01418-8.
37. Tshori S, Livschitz S, Volodarsky I, Fabrikant J, George J. Evaluation of ATTR-cardiac amyloidosis employing Tc-99m pyrophosphate scintigraphy using planar, SPECT and gated SPECT imaging on dedicated cardiac CZT camera. Eur Heart J. 2020;41(Supplement_2):2020.

38. Sikanderkhel S, Liu Y-H, Liu C, Miller E. Suv quantification of 99Mtc-Pyp Imaging in Ttr-cardiac amyloidosis using a Czt camera: a new tool in the armamentarium. J Am Coll Cardiol [Internet]. 2018;71(11):A1689. https://doi.org/10.1016/S0735-1097(18)32230-7.
39. Dorbala S, Park MA, Cuddy S, Singh V, Sullivan K, Kim S, et al. Absolute quantitation of cardiac 99mTc-pyrophosphate using cadmium-zinc-telluride-based SPECT/CT. J Nucl Med. 2021;62(5):716–22.
40. Quarta CC, Solomon SD, Uraizee I, Kruger J, Longhi S, Ferlito M, et al. Left ventricular structure and function in transthyretin-related versus light-chain cardiac amyloidosis. Circulation. 2014;129(18):1840–9.
41. Phelan D, Collier P, Thavendiranathan P, Popović ZB, Hanna M, Plana JC, et al. Relative apical sparing of longitudinal strain using two-dimensional speckle-tracking echocardiography is both sensitive and specific for the diagnosis of cardiac amyloidosis. Heart. 2012;98(19):1442–8.
42. Koyama J, Falk RH. Prognostic significance of strain doppler imaging in light-chain amyloidosis. JACC Cardiovasc Imaging [Internet]. 2010;3(4):333–42. https://doi.org/10.1016/j.jcmg.2009.11.013.
43. Senapati A, Sperry BW, Grodin JL, Kusunose K, Thavendiranathan P, Jaber W, et al. Prognostic implication of relative regional strain ratio in cardiac amyloidosis. Heart. 2016;102(10):748–54.
44. Bellavia D, Pellikka PA, Dispenzieri A, Scott CG, Al-Zahrani GB, Grogan M, et al. Comparison of right ventricular longitudinal strain imaging, tricuspid annular plane systolic excursion, and cardiac biomarkers for early diagnosis of cardiac involvement and risk stratification in primary systematic (AL) amyloidosis: a 5-year cohort stud. Eur Heart J Cardiovasc Imaging. 2012;13(8):680–9.
45. Cappelli F, Porciani MC, Bergesio F, Perlini S, Attanà P, Pignone AM, et al. Right ventricular function in AL amyloidosis: characteristics and prognostic implication. Eur Heart J Cardiovasc Imaging. 2012;13(5):416–22.
46. Patel AR, Dubrey SW, Mendes LA, Skinner M, Cupples A, Falk RH, et al. Right ventricular dilation in primary amyloidosis: an independent predictor of survival. Am J Cardiol. 1997;80(4):486–92.
47. Syed IS, Glockner JF, Feng DL, Araoz PA, Martinez MW, Edwards WD, et al. Role of cardiac magnetic resonance Imaging in the detection of cardiac amyloidosis. JACC Cardiovasc Imaging [Internet]. 2010;3(2):155–64. https://doi.org/10.1016/j.jcmg.2009.09.023.
48. Fontana M, Pica S, Reant P, Abdel-Gadir A, Treibel TA, Banypersad SM, et al. Prognostic value of late gadolinium enhancement cardiovascular magnetic resonance in cardiac amyloidosis. Circulation. 2015;132(16):1570–9.
49. Zhao L, Tian Z, Fang Q. Diagnostic accuracy of cardiovascular magnetic resonance for patients with suspected cardiac amyloidosis: a systematic review and meta-analysis. BMC Cardiovasc Disord [Internet]. 2016;16(1):1–10. https://doi.org/10.1186/s12872-016-0311-6.
50. Fontana M, Banypersad SM, Treibel TA, Maestrini V, Sado DM, White SK, et al. Native T1 mapping in transthyretin amyloidosis. JACC Cardiovasc Imaging. 2014;7(2):157–65.
51. Banypersad SM, Sado DM, Flett AS, Gibbs SDJ, Pinney JH, Maestrini V, et al. Quantification of myocardial extracellular volume fraction in systemic AL amyloidosis: an equilibrium contrast cardiovascular magnetic resonance study. Circ Cardiovasc Imaging. 2013;6(1):34–9.
52. Mongeon FP, Jerosch-Herold M, Coelho-Filho OR, Blankstein R, Falk RH, Kwong RY. Quantification of extracellular matrix expansion by CMR in infiltrative heart disease. JACC Cardiovasc Imaging [Internet]. 2012;5(9):897–907. https://doi.org/10.1016/j.jcmg.2012.04.006.
53. Fontana M, Banypersad SM, Treibel TA, Maestrini V, Sado D, White SK, et al. AL and ATTR cardiac amyloid are different: native T1 mapping and ECV detect different biology. J Cardiovasc Magn Reson. 2014;16(S1):1–2.
54. Hutt DF, Fontana M, Burniston M, Quigley AM, Petrie A, Ross JC, et al. Prognostic utility of the Perugini grading of 99m Tc-DPD scintigraphy in transthyretin (ATTR) amyloidosis and its relationship with skeletal muscle and soft tissue amyloid. Eur Heart J Cardiovasc Imaging. 2017;18(12):1344–50.

55. Yamamoto Y, Onoguchi M, Haramoto M, Kodani N, Komatsu A, Kitagaki H, et al. Novel method for quantitative evaluation of cardiac amyloidosis using 201TlCl and 99mTc-PYP SPECT. Ann Nucl Med. 2012;26(8):634–43.
56. Castano A, Haq M, Narotsky DL, Goldsmith J, Weinberg RL, Morgenstern R, et al. Multicenter study of planar technetium 99m pyrophosphate cardiac Imaging: predicting survival for patients with ATTR cardiac amyloidosis. JAMA Cardiol. 2016;1(8):880–9.
57. Sperry BW, Vranian MN, Tower-Rader A, Hachamovitch R, Hanna M, Brunken R, et al. Regional variation in technetium pyrophosphate uptake in transthyretin cardiac amyloidosis and impact on mortality. JACC Cardiovasc Imaging. 2018;11(2):234–42.
58. Ramsay SC, Cuscaden C. The current status of quantitative SPECT/CT in the assessment of transthyretin cardiac amyloidosis. J Nucl Cardiol [Internet]. 2019; https://doi.org/10.1007/s12350-019-01935-1.
59. Minutoli F, Di Bella G, Mazzeo A, Laudicella R, Gentile L, Russo M, et al. Serial scanning with 99mTc-3, 3-diphosphono-1, 2-propanodicarboxylic acid (99mTc-DPD) for early detection of cardiac amyloid deposition and prediction of clinical worsening in subjects carrying a transthyretin gene mutation. J Nucl Cardiol [Internet]. 2019; https://doi.org/10.1007/s12350-019-01950-2.
60. Castaño A, DeLuca A, Weinberg R, Pozniakoff T, Blaner WS, Pirmohamed A, et al. Serial scanning with technetium pyrophosphate (99mTc-PYP) in advanced ATTR cardiac amyloidosis. J Nucl Cardiol. 2016;23(6):1355–63.
61. Martinez-Naharro A, Abdel-Gadir A, Treibel TA, Zumbo G, Knight DS, Rosmini S, et al. CMR-verified regression of cardiac AL amyloid after chemotherapy. JACC Cardiovasc Imaging [Internet]. 2018;11(1):152–4. https://doi.org/10.1016/j.jcmg.2017.02.012.
62. Slart RHJA, Glaudemans AWJM, Hazenberg BPC, Noordzij W. Imaging cardiac innervation in amyloidosis. J Nucl Cardiol. 2019;26(1):174–87.
63. Jonker DL, Hazenberg BPC, Nienhuis HLA, Slart RHJA, Glaudemans AWJM, Noordzij W. Imaging cardiac innervation in hereditary transthyretin (ATTRm) amyloidosis: a marker for neuropathy or cardiomyopathy in case of heart failure? J Nucl Cardiol [Internet]. 2018; https://doi.org/10.1007/s12350-018-01477-y.
64. Flotats A, Carrió I, Agostini D, Le Guludec D, Marcassa C, Schaffers M, et al. Proposal for standardization of 123I-metaiodobenzylguanidine (MIBG) cardiac sympathetic imaging by the EANM cardiovascular committee and the European Council of Nuclear Cardiology. Eur J Nucl Med Mol Imaging. 2010;37(9):1802–12.
65. Pontico M, Brunotti G, Conte M, Corica F, Cosma L, De Angelis C, et al. The prognostic value of 123I-mIBG SPECT cardiac imaging in heart failure patients: a systematic review. J Nucl Cardiol [Internet]. 2021; https://doi.org/10.1007/s12350-020-02501-w.
66. Wan N, Travin MI. Cardiac Imaging with 123I-meta-iodobenzylguanidine and Analogous PET tracers: current status and future perspectives. Semin Nucl Med [Internet]. 2020;50(4):331–48. https://doi.org/10.1053/j.semnuclmed.2020.03.001.
67. Hongo M, Urushibata K, Kai R, Takahashi W, Koizumi T, Uchikawa S, et al. Iodine-123 metaiodobenzylguanidine scintigraphic analysis of myocardial sympathetic innervation in patients with AL (primary) amyloidosis. Am Heart J. 2002;144(1):122–9.
68. Lekakis J, Dimopoulos MA, Prassopoulos V, Mavrikakis M, Gerali S, Sifakis N, et al. Myocardial adrenergic denervation in patients with primary (AL) amyloidosis. Amyloid. 2003;10(2):117–20.
69. Noordzij W, Glaudemans AWJM, Van Rheenen RWJ, Hazenberg BPC, Tio RA, Dierckx RAJO, et al. 123I-labelled metaiodobenzylguanidine for the evaluation of cardiac sympathetic denervation in early stage amyloidosis. Eur J Nucl Med Mol Imaging. 2012;39(10):1609–17.
70. Nakajima K, Matsumoto N, Kasai T, Matsuo S, Kiso K, Okuda K. Normal values and standardization of parameters in nuclear cardiology: Japanese society of nuclear medicine working group database. Ann Nucl Med. 2016;30(3):188–99.

71. Gill JS, Hunter GJ, Gane G, Camm AJ. Heterogeneity of the human myocardial sympathetic innervation: in vivo demonstration by iodine 123-labeled meta-iodobenzylguanidine scintigraphy. Am Heart J. 1993;126(2):390–8.
72. Jacobson AF, Senior R, Cerqueira MD, Wong ND, Thomas GS, Lopez VA, et al. Myocardial Iodine-123 meta-Iodobenzylguanidine Imaging and cardiac events in heart failure. Results of the prospective ADMIRE-HF (AdreView myocardial Imaging for risk evaluation in heart failure) study. J Am Coll Cardiol [Internet]. 2010;55(20):2212–21. https://doi.org/10.1016/j.jacc.2010.01.014.
73. Coutinho MCA, Cortez-Dias N, Cantinho G, Conceição I, Oliveira A, Bordalo E, Sá A, et al. Reduced myocardial 123-iodine metaiodobenzylguanidine uptake: a prognostic marker in familial amyloid polyneuropathy. Circ Cardiovasc Imaging. 2013;6(5):627–36.
74. Coutinho CA, Conceição I, Almeida A, Cantinho G, Sargento L, Vagueiro MC. Early detection of sympathetic myocardial denervation in patients with familial amyloid polyneuropathy type I. Rev Port Cardiol [Internet]. 2004;23(2):201–11. http://europepmc.org/abstract/MED/15116456
75. Phull P, Sanchorawala V, Connors LH, Doros G, Ruberg FL, Berk JL, et al. Monoclonal gammopathy of undetermined significance in systemic transthyretin amyloidosis (ATTR). Amyloid [Internet]. 2018;25(1):62–7. https://doi.org/10.1080/13506129.2018.1436048.
76. Gallini C, Tutino F, Martone R, Ciaccio A, Costanzo EN, Taborchi G, et al. Semi-quantitative indices of cardiac uptake in patients with suspected cardiac amyloidosis undergoing 99mTc-HMDP scintigraphy. J Nucl Cardiol [Internet]. 2021;28(1):90–9. https://doi.org/10.1007/s12350-019-01643-w.
77. Ramsay SC, Lindsay K, Fong W, Patford S, Younger J, Atherton J. Tc-HDP quantitative SPECT/CT in transthyretin cardiac amyloid and the development of a reference interval for myocardial uptake in the non-affected population. Eur J Hybrid Imaging. 2018;2(1):1–13.
78. Scully PR, Morris E, Patel KP, Treibel TA, Burniston M, Klotz E, et al. DPD quantification in cardiac amyloidosis: a novel Imaging biomarker. JACC Cardiovasc Imaging. 2020;13(6):1353–63.
79. Miller RJH, Cadet S, Mah D, Pournazari P, Chan D, Fine NM, et al. Diagnostic and prognostic value of technetium-99m pyrophosphate uptake quantitation for transthyretin cardiac amyloidosis. J Nucl Cardiol [Internet]. 2021;28(5):1835–45. https://doi.org/10.1007/s12350-021-02563-4.
80. Bravo PE, Di Carli MF, Dorbala S. Role of PET to evaluate coronary microvascular dysfunction in non-ischemic cardiomyopathies. Heart Fail Rev. 2017;22(4):455–64.
81. Dorbala S, Vangala D, Bruyere J, Quarta C, Kruger J, Padera R, et al. Coronary microvascular dysfunction is related to abnormalities in myocardial structure and function in cardiac amyloidosis. JACC Hear Fail. 2014;2(4):358–67.
82. Migrino RQ, Truran S, Gutterman DD, Franco DA, Bright M, Schlundt B, et al. Human microvascular dysfunction and apoptotic injury induced by AL amyloidosis light chain proteins. Am J Physiol Heart Circ Physiol. 2011;301(6):2305–12.
83. Al Suwaidi J, Velianou JL, Gertz MA, Cannon RO, Higano ST, Holmes DR, et al. Systemic amyloidosis presenting with angina pectoris. Ann Intern Med. 1999;131(11):838–41.
84. Morgenstern R, Yeh R, Castano A, Maurer MS, Bokhari S. 18Fluorine sodium fluoride positron emission tomography, a potential biomarker of transthyretin cardiac amyloidosis. J Nucl Cardiol. 2018;25(5):1559–67.
85. Martineau P, Finnerty V, Giraldeau G, Authier S, Harel F, Pelletier-Galarneau M. Examining the sensitivity of 18F-NaF PET for the imaging of cardiac amyloidosis. J Nucl Cardiol. 2021;28:209–18.
86. Zhang LX, Martineau P, Finnerty V, Giraldeau G, Parent MC, Harel F, et al. Comparison of 18F-sodium fluoride positron emission tomography imaging and 99mTc-pyrophosphate in cardiac amyloidosis. J Nucl Cardiol. 2022;29:1132–40.

87. Kim YJ, Ha S, Kim Y, il. Cardiac amyloidosis imaging with amyloid positron emission tomography: a systematic review and meta-analysis. J Nucl Cardiol [Internet]. 2020;27(1):123–32. https://doi.org/10.1007/s12350-018-1365-x.
88. Antoni G, Lubberink M, Estrada S, Axelsson J, Carlson K, Lindsjö L, et al. In vivo visualization of amyloid deposits in the heart with 11C-PIB and PET. J Nucl Med. 2013;54(2):213–20.
89. Rosengren S, Skibsted Clemmensen T, Tolbod L, Granstam SO, Eiskjær H, Wikström G, et al. Diagnostic accuracy of [11C]PIB positron emission tomography for detection of cardiac amyloidosis. JACC Cardiovasc Imaging. 2020;13(6):1337–47.
90. Dorbala S, Vangala D, Semer J, Strader C, Bruyere JR, Di Carli MF, et al. Imaging cardiac amyloidosis: a pilot study using 18F-florbetapir positron emission tomography. Eur J Nucl Med Mol Imaging. 2014;41(9):1652–62.
91. Osborne DR, Acuff SN, Stuckey A, Wall JS. A routine PET/CT protocol with streamlined calculations for assessing cardiac amyloidosis using 18F-florbetapir. Front Cardiovasc Med. 2015;2(May):1–9.
92. Law WP, Wang WYS, Moore PT, Mollee PN, Ng ACT. Cardiac amyloid imaging with 18F-Florbetaben PET: a pilot study. J Nucl Med. 2016;57(11):1733–9.
93. Genovesi D, Vergaro G, Giorgetti A, Marzullo P, Scipioni M, Santarelli MF, et al. [18F]-Florbetaben PET/CT for differential diagnosis among cardiac immunoglobulin light chain, transthyretin amyloidosis, and mimicking conditions. JACC Cardiovasc Imaging. 2021;14(1):246–55.
94. Kircher M, Ihne S, Brumberg J, Morbach C, Knop S, Kortüm KM, et al. Detection of cardiac amyloidosis with 18F-Florbetaben-PET/CT in comparison to echocardiography, cardiac MRI and DPD-scintigraphy. Eur J Nucl Med Mol Imaging. 2019;46(7):1407–16.